Study of Peak-to-Peak Amplitude Distribution in Cardiac Rhythms: Electrophysiological Mapping in Langendorff-Perfused Rabbit Hearts

José Carlos Gomes Junior[1], Jimena Gabriela Siles Paredes[1], Tainan Cerqueira Neves[1], Angélica Drielly Santos de Quadros[1], Saleem Ullah[1], Vinícius de Paula Silva[1], João Loures Salinet Júnior[1]

[1]HEartLab, Federal University of ABC, São Bernardo do Campo, Brazil

Abstract

Cardiovascular diseases are the leading cause of global mortality, with cardiac arrhythmias posing a significant challenge due to their complex electrophysiological substrates. This study characterized peak-to-peak amplitude distributions across epicardial regions (right atrium, left atrium, and ventricle) during sinus rhythm (SR), atrial tachycardia (AT), ventricular fibrillation (VF), and SR with atrioventricular block (AVB) using Langendorff-perfused rabbit hearts. Silver, silver/iridium and platinum microelectrode arrays (MEAs) were employed for invasive electrical mapping, with signal processing (60 Hz notch filter, 0.5–250 Hz bandpass) and MATLAB® analysis. The results revealed a unipolar voltage cutoff of 2.74 mV (RA), 2.64 mV (LA), and 7.71 mV (V), and a bipolar cutoff of 0.92 mV (RA), 0.98 mV (LA), and 4.57 mV (V), calculated using the 95th percentile during SR. In comparing the rhythms, the median peak-to-peak amplitudes in VF decreased tenfold compared to SR, while those in AT were preserved. The MEAs made of platinum exhibited the highest peak-to-peak amplitudes, with a median value 297.7% greater compared to MEAs made of pure silver. These results contribute to refining voltage mapping approaches in experimental cardiac models.

1. Introduction

Cardiovascular diseases (CVDs) are the leading cause of global mortality, accounting for 32% of deaths in 2022 [1]. Among these, cardiac arrhythmias stand out for their complexity and clinical impact, such as atrial fibrillation (AF), which increases the risk of stroke fivefold [2]. Electrical and structural cardiac remodeling, common in infarctions and fibrosis, creates arrhythmogenic substrates (low-voltage areas and heterogeneity) that perpetuate ventricular and atrial arrhythmias, increasing morbidity and mortality [3,4].

Voltage mapping emerges as an essential tool for identifying arrhythmogenic tissue by characterizing critical regions through signal amplitudes. Electroanatomic systems (e.g., CARTO 3) record local potentials, detecting low-voltage areas (<0.5 mV) associated with fibrosis and slow conduction [5]. Peak-to-peak amplitude analyses discriminate healthy tissue (e.g., >1.5 mV) from pathological zones, guiding interventions like ablation with spatial precision [6,7].

In this study, we evaluated the distribution of peak-to-peak amplitudes in epicardial regions (atria and ventricle) during sinus rhythm (SR), sinus rhythm with atrioventricular nodal block (AVB), atrial tachycardia (AT) and ventricular fibrillation (VF) using an experimental model with Langendorff-perfused rabbit hearts. We used different microelectrode arrays (MEAs) of silver, silver/iridium and platinum for unipolar signal acquisition (4 kHz), processed by digital filtering (notch 60 Hz, bandpass 0.5-250 Hz) and MATLAB® analysis.

2. Material and Methods

2.1. Animal Model Experiments

The conducted studies were approved by the Animal Use Ethics Committee (CEUA) of the Federal University of ABC (UFABC) under protocol number 3947230519. A total of 9 New Zealand rabbits (3.44 ± 0.36 kg) were used in this study, anesthetized with Buprenorphine (0.05 mg/kg, IM) followed by an intramuscular injection of the Ketamine/Xylazine cocktail after 30 minutes (50 mg/kg and 7 mg/kg, respectively) to induce deep anesthesia, followed by heparinization (500 U/kg, IV) and euthanasia by thoracotomy for heart extraction. The hearts were perfused in a Langendorff system with modified Krebs-Henseleit solution (37.5-38°C, pH 7.6 ± 0.09, bubbled with carbogen) under constant pressure (70-80 mmHg), with contractility suppression by (-)-blebbistatin (25 μM initial, 1.7 μM continuous).

To obtain different heart rhythms, arrhythmias were induced via programmed stimulation protocols (S1-S1/S1-S2) and carbachol perfusion (1 μM), while the atrioventricular (AV) node was ablated with radiofrequency (15 W) to isolate atrial signals, when required.

2.2. Cardiac Mapping

Cardiac mapping was performed through invasive epicardial mapping using three microelectrode arrays (MEAs) per experiment, positioned in the right atrium (RA), left atrium (LA), and ventricle (V). The MEAs were fabricated from polyethylene terephthalate (PET) with microelectrodes made of silver (Ag), silver/iridium (Ag/Ir), or platinum (Pt). Unipolar signals were acquired at 4 kHz, using the aorta as a reference, with amplification provided by Intan Technologies amplifiers and the Open Ephys system. To ensure efficient electrical contact in the atria, balloons were inserted to increase atrial volume and expand the contact surface between the epicardial tissue and the MEA. In total, 7 MEAs were used across different experiments: 3 MEAs with Pt microelectrodes, 2 MEAs with Ag/Ir microelectrodes, and 2 MEAs with Ag microelectrodes.

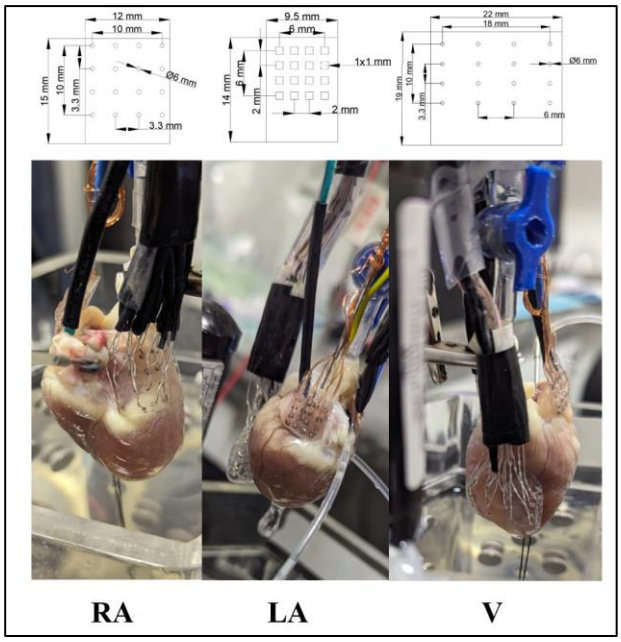

Figure 1. Figure 1 displays the MEAs and their schematic diagrams (top). While both the RA and LA MEAs are positioned in their corresponding epicardial regions, the V MEA is placed between the right and left ventricles (bottom). Each of the three MEAs contains a total of 16 electrodes.

2.3. Signal Analysis

The unipolar signals were processed with a focus on preserving activation and recovery amplitudes, which are essential for voltage mapping. The processing pipeline included: (1) conversion to µV with a 60 dB gain, (2) linear trend removal (detrending), (3) a 60 Hz notch filter to eliminate powerline interference, (4) a bandpass filter (0.5–250 Hz) to retain physiological components, and (5) derivation of bipolar signals for the calculation of the voltage cutoff value during SR. The post-processed signals were analysed in MATLAB®, peaks were manually selected, and peak-to-peak amplitudes were calculated.

To determine the voltage cutoff values for healthy tissue, recordings from hearts (n = 4) in SR without drug influence, taken at the beginning of the perfusions, were used, applying the 95th percentile [8] on MEAs with silver microelectrodes. For the amplitude analysis across different rhythms, 3 hearts were studied, comparing the median peak-to-peak amplitudes of the RA, LA, and V between arrhythmias and SR, with each comparison performed within the same heart. Finally, a total of 9 SR recordings from the LA were used to analyse the influence of microelectrode material: 3 hearts for Ag, 3 hearts for Ag/Ir, and 3 hearts for Pt. In total, 9 LA recordings were analysed.

3. Results

The analysis of the influence of MEA microelectrode material demonstrated distinct differences in the peak-to-peak amplitude of LA signals between the materials studied. Figure 2 shows the histogram of the peak-to-peak amplitude distribution of unipolar sinus rhythm LA signals (n = 9 hearts): 3 samples recorded with MEAs with Ag microelectrodes, 3 with Ag/Ir, and 3 with Pt. All signals were analyzed using a 5-second window. For Ag, the median found was 9.0 mV (mean 10.1 ± 6.7 mV); for Ag/Ir, approximately 20.6 mV (18.5 ± 12.3 mV); and, finally, for Pt, it was 26.9 mV (27.7 ± 11.4 mV).

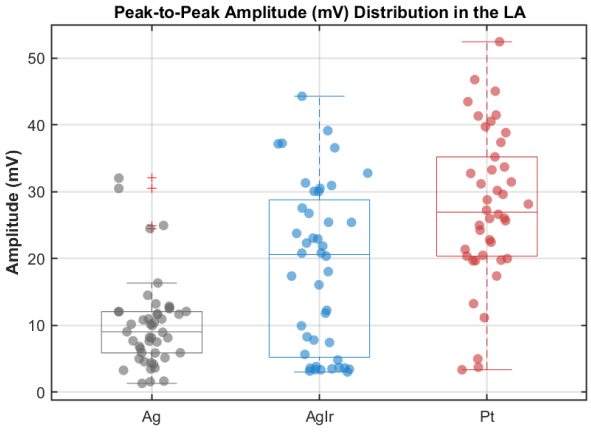

Figure 2. Box plot of peak-to-peak amplitude distribution analysis in the LA region, SR-type signal. Ag – silver (gray); Ag/Ir – silver/iridium (blue); Pt – platinum (red). Each point represents a microelectrode.

The voltage cutoff values (95th percentile) for healthy epicardial tissue of the RA, LA, and V, determined (Table

1) for unipolar and bipolar signals, were obtained through peak-to-peak amplitude within a 5-second window. Four hearts in SR were analyzed, with measured cycle lengths (CL) of 528.48 ± 5.71 ms in the RA, 528.25 ± 16.03 ms in the LA, and 521.30 ± 0.01 ms in the V.

Table 1. Unipolar and bipolar voltage cutoff values for healthy tissue in SR from the RA, LA, and V.

Signal	RA (mV)	LA (mV)	V (mV)
Unipolar	2.74	2.64	7.71
Bipolar	0.92	0.98	4.57

The mean and standard deviation found for unipolar signals were: 8.65 ± 8.58 mV for the RA, 13.75 ± 10.10 mV for the LA, and 15.36 ± 8.78 mV for the V. For bipolar signals: 11.01 ± 9.60 mV for the RA, 14.36 ± 7.20 mV for the LA, and 11.50 ± 5.30 mV for the V. All analyses were performed on signals recorded using MEAs with pure silver microelectrodes.

Finally, the analysis of peak-to-peak amplitude variability among different cardiac rhythms with SR in presented in (Table 2), signals from 3 hearts were analyzed: 1 signal of VF rhythm (cycle length 542.20 ms in RA, 540.37 ms in LA, and 170.56 ms in V), 1 signal of AT rhythm (cycle length 360.60 ms in RA, 351.68 ms in LA, and 914.37 ms in V), and 1 signal under the AVB condition (cycle length 607.80 ms in RA and 606.42 ms in LA). In all analyses, the medians of the peak-to-peak amplitudes from the RA, LA, and V chambers were compared within a 5-second window.

The analyses of hearts 1 and 2 had the following MEA microelectrode material configuration: Ag for RA and V, and Ag/Ir for LA. For the analysis of heart 3, the configuration was: Ag/Ir for RA and LA, and Ag for V.

Table 2. Median peak-to-peak amplitude variability among different cardiac rhythms. on the right is the median for SR, and on the left is the median for the arrhythmia.

	RA (mV)		LA (mV)		V (mV)	
Analysis	SR	VF	SR	VF	SR	VF
Heart 1	5.5	3.3	25	6.1	21	2.0
Analysis	SR	AT	SR	AT	SR	AT
Heart 2	3.70	3.20	23.8	25.5	12.4	11.7
Analysis	SR	AVB	SR	AVB	SR	AVB
Heart 3	3.7	2.6	4.8	1.1	2.5	0.6

4. Discussion

Regarding the analysis of the influence of MEA material, it was observed that among Ag, Ag/Ir, and Pt, the values related to Pt showed the highest peak-to-peak amplitude, with Pt exhibiting a 297.7% higher amplitude compared to pure silver. This result is supported by the fact that platinum has characteristics of high biocompatibility, mechanical strength, and, most importantly, good electrical conductivity, making it a material widely used in clinical practice in the field of electrocardiology [9–11].

Regarding the determination of epicardial voltage cutoff values for healthy tissue using the 95th percentile, the values found for the rabbit animal model are logically consistent with those reported for humans [12]: unipolar signal values are higher than bipolar ones, and the RA and LA chambers show similar values (2.74 mV and 2.64 mV for unipolar; 0.92 mV and 0.98 mV for bipolar). The signals were analyzed during SR, and the cycle length was calculated as 528.48 ± 5.71 ms for RA, 528.25 ± 16.03 ms for LA, and 521.30 ± 0.01 ms for V, all within the physiological range for rabbits [13]. The absence of histological confirmation represents a limitation, as subclinical structural changes could influence these thresholds, and the values were determined for an animal model.

The comparative analysis of peak-to-peak amplitude (median) variability between arrhythmias and SR revealed that in the disorganized rhythm of VF, the peak-to-peak amplitudes decreased compared to SR in the chamber of the arrhythmia—the ventricle—by a factor of 10. In contrast, for AT, a more organized rhythm, the peak-to-peak amplitude was preserved. In the condition of AV nodal block, the absence of electrical activity in the ventricles showed an amplitude around 0.6 mV, consistent with and similar to values corresponding to the absence of activity in voltage mapping. These findings support the well-known relationship between loss of cellular synchrony and amplitude reduction, although limitations such as the small sample size and the controlled Langendorff conditions must be acknowledged.

High standard deviations in peak-to-peak amplitudes reflect the variability of the Langendorff model, exacerbated by the non-uniform fixation of MEAs, differences in electrode materials (Ag vs. Ag/Ir vs. Pt), tissue heterogeneity, and perfusion variations. Paired analysis (same heart under different rhythms) minimized interindividual variability, strengthening data robustness, although model limitations—such as potential blebbistatin effects and differences between ex vivo and in vivo conditions—highlight the need for further validation in contexts closer to real physiology.

5. Conclusion

This study characterized peak-to-peak amplitude distributions across epicardial regions in Langendorff-perfused rabbit hearts, revealing rhythm- and material-dependent electrophysiological patterns. Organized rhythms such as AT preserved atrial amplitudes, whereas disorganized rhythms like VF caused marked reductions, and AV block showed near-absent ventricular activity. Platinum MEAs exhibited the highest amplitudes, 297.7% greater than pure silver, highlighting the critical influence

of electrode material on signal fidelity. The voltage cutoff values determined for healthy tissue were consistent with human data, with unipolar signals exceeding bipolar ones and similar RA and LA values. High variability, due to model-specific factors such as tissue heterogeneity, MEA fixation, perfusion differences, and electrode material, underscores the need for optimized protocols and larger sample sizes. Paired intra-heart analyses enhanced robustness, but limitations—including small sample size, absence of histological validation, and ex vivo conditions—point to the need for further studies under conditions closer to physiological reality. Overall, these findings refine epicardial voltage mapping approaches and provide insight into arrhythmia-specific electrical desynchrony in experimental models.

Acknowledgments

José Carlos Gomes Junior is supported by Coordination for the Improvement of Higher Education Personnel – Brazil (CAPES – Funding Code 001: Ordinance No. 206 of September 4, 2018). Jimena Gabriela Siles Paredes is supported by grant #2020/03601-9, Sao Paulo Research Foundation (FAPESP). Tainan Cerqueira Neves and Angélica Drielly Santos de Quadros are supported by FAPESP grant #2024/02521-2 and #2023/06306-6, respectively. João Loures Salinet Júnior are supported by grant #2018/25606-2, Sao Paulo Research Foundation (FAPESP).

References

[1] World Health Organization, "Cardiovascular Diseases (CVDs)," Newsroom, Fact sheets, Detail, Cardiovascular diseases (CVDs), Jul. 2025. [Online].

[2] T. K. Patel and R. S. Passman, "Atrial Fibrillation and Stroke: The Evolving Role of Rhythm Control," *Curr. Treat. Options Cardiovasc. Med*., vol. 15, no. 3, pp. 299–312, Feb. 2013.

[3] Z. Aziz *et al*., "Targeted ablation of ventricular tachycardia guided by wavefront discontinuities during sinus rhythm: a new functional substrate mapping strategy," *Circulation*, vol. 140, no. 16, pp. 1383–1397, Oct. 2019.

[4] K. Nademanee, E. Lockwood, N. Oketani, and B. Gidney, "Catheter ablation of atrial fibrillation guided by complex fractionated atrial electrogram mapping of atrial fibrillation substrate," *J. Cardiol*., vol. 55, no. 3, pp. 1–12, May 2010.

[5] B. Pathik *et al*., "High-resolution mapping demonstrates conduction and substrate variability in right atrial macro-re-entrant tachycardia," *JACC: Clin. Electrophysiol*., vol. 3, no. 9, pp. 971–986, Sep. 2017.

[6] D. Ragot *et al*., "Unipolar electrogram-based voltage mapping with far-field cancellation to improve detection of abnormal atrial substrate during atrial fibrillation," *J. Cardiovasc. Electrophysiol.*, vol. 32, no. 6, pp. 1572–1583, Jun. 2021.

[7] O. Berenfeld *et al.*, "Time- and frequency-domain analyses of atrial fibrillation activation rate: The optical mapping reference," *Heart Rhythm*, vol. 8, no. 11, pp. 1758–1765, Nov. 2011.

[8] M. D. Hutchinson *et al.*, "Endocardial Unipolar Voltage Mapping to Detect Epicardial Ventricular Tachycardia Substrate in Patients with Nonischemic Left Ventricular Cardiomyopathy," *Circ. Arrhythm. Electrophysiol.*, vol. 4, no. 1, pp. 49–55, Feb. 2011.

[9] A. N. Dalrymple *et al.*, "Electrochemical and biological characterization of thin-film platinum-iridium alloy electrode coatings: a chronic in vivo study," *J. Neural Eng.*, vol. 17, no. 3, Jun. 2020.

[10] M. Linhart *et al.*, "In vitro comparison of platinum–iridium and gold tip electrodes: lesion depth in 4 mm, 8 mm, and irrigated-tip radiofrequency ablation catheters," *Europace*, vol. 11, no. 5, pp. 565–570, May 2009.

[11] M. Stühlinger *et al.*, "Gold Versus Platinum in AVNRT Ablation: Gold Alloy Versus Platinum–Iridium Electrode for Ablation of AVNRT," *J. Cardiovasc. Electrophysiol.*, vol. 19, no. 3, pp. 242–246, Mar. 2008.

[12] N. Denham *et al.*, "Electrotomographic mapping with principal component referenced unipoles and perpendicular bipoles," *Heart Rhythm*, vol. 22, no. 7, pp. 1843–1853, Jul. 2025.

[13] Electrocardiography of Laboratory Animals, 2nd ed. Elsevier, 2019. ISBN 978-0-12-809469-3, DOI: https://doi.org/10.1016/C2015-0-05761-6.

Address for correspondence:

José Carlos Gomes Junior
HEartLab - Biomedical Engineering - CECS
Federal University of ABC - UFABC
Street: Al. da Universidade, S/N, Zeta Building, L107, São Bernardo do Campo - SP, Brazil
Email: junior.gomes@ufabc.edu.br